

A Theoretical Study of the Mechanism for the Reductive Half-Reaction of Pea Seedling Amine Oxidase (PSAO)

Rajeev Prabhakar and Per E. M. Siegbahn*

Department of Physics, Stockholm University, Box 6730, S-113 85 Stockholm, Sweden

Received: September 18, 2000; In Final Form: February 28, 2001

On the basis of a large amount of experimental information, the reductive half-reaction of PSAO has been studied quantum mechanically using hybrid density functional theory (B3LYP). The suggested mechanism agrees very well with the one suggested experimentally and incorporates the observation of two different Schiff bases. The half-reaction is suggested to occur in six steps, and transition state structures connecting the different intermediates have been optimized. Two of these steps are further subdivided into two separate parts. The rate-limiting step is found to be the C–H activation of the substrate in agreement with experimental findings, and this step is found to be driven by a large gain of aromaticity in the TPQ ring. To make full use of this driving force, O₂ of TPQ is suggested to be protonated prior to the C–H activation. A mechanism for how this protonation might occur is suggested. The roles of the TPQ cofactor and the critical Asp300 are discussed and compared to experimental observations and suggestions.

I. Introduction

Copper-containing amine oxidases (CAO's) form a family of redox active enzymes which is present in both prokaryotes and eukaryotes. They catalyze the oxidative deamination of primary amines by dioxygen to form aldehydes, ammonia, and hydrogen peroxide. In prokaryotes, amine oxidases provide the source of carbon and nitrogen but in eukaryotes they are suggested to be involved in cell differentiation, cell growth, detoxification, wound healing, cell signaling, and possibly in cell death.^{1–5} The medical interest in amine oxidases is increasing, with reports suggesting their involvement as a mediator in the interaction between lymphocytes and endothelial cells,⁶ in the formation of vascular plaques suggested to be involved in congestive heart failure,⁷ and in vascular damage observed in late-diabetic complications.⁸ The CAO enzymes are homodimeric with 70–95 kDa subunits, and with each subunit containing one copper center.^{5,9,10} The catalytic reaction requires a redox cofactor, 2,4,5-trihydroxyphenylalaninequinone referred to as a topa quinone (TPQ), which is ubiquitous in amine oxidases. The presence of TPQ has been confirmed in the amine oxidases in pea seedling (PSAO),¹¹ in pig kidney (PKAO),¹² in *Escherichia coli* (ECAO),¹³ in *Arthobacter PI* (APAO),¹⁴ in bovine serum (BSAO),¹⁵ and in yeast (*Hansenula polymorpha*).¹⁶ Two hypotheses have been advanced for the biogenesis of the TPQ cofactor, involving either a self-processing mechanism oxidizing a tyrosine residue into TPQ^{17,18} or a direct incorporation of it into the enzyme via a unique tRNA.¹⁵ It is possible that the copper center therefore could play a crucial, dual role in amine oxidases. Not only is the copper atom suggested to be involved in the biogenesis of the organic quinone cofactor, but it is also instrumental in the catalytic oxidation of amines in the enzyme. Most amine oxidases are substrate specific; prokaryotic bacterial amine oxidases and mammalian plasma oxidases prefer monoamines as substrates, whereas PSAO has stronger preference for diamines. The catalytic mechanism of copper-dependent amine oxidases has recently been reviewed.^{19,20}

Experiments strongly suggest that all CAOs utilize a two step, ping-pong type mechanism in its catalytic cycle. The process

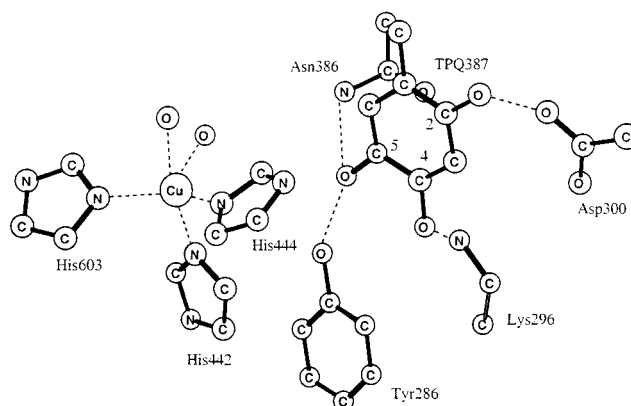
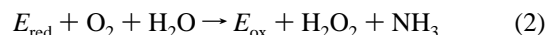


Figure 1. X-ray structure of the active site region of PSAO.

can be formally divided into reductive and oxidative half-reactions, with the reductive half-reaction being



and with the oxidative half-reaction being



This type of mechanism is supported by steady-state kinetics for the CAOs with regard to amine substrate and dioxygen.^{1,21} Kinetic constants obtained for the reduction of the enzyme in the absence of dioxygen agree well with the steady-state parameters for the reductive half-reaction.²² The rates of these two half-reactions depend on the source of enzyme with the rate for the reductive half-reaction found to be much greater than the one for the oxidative half-reaction for plant amine oxidases while the opposite is true for pig plasma amine oxidase (PPAO).^{23,24}

The crystal structure for eukaryotic PSAO has been solved to 2.2 Å resolution.²⁵ Each monomer in PSAO contains three domains. At the active site, see Figure 1, the Cu atom is coordinated to the imidazole side-chains of three histidines,

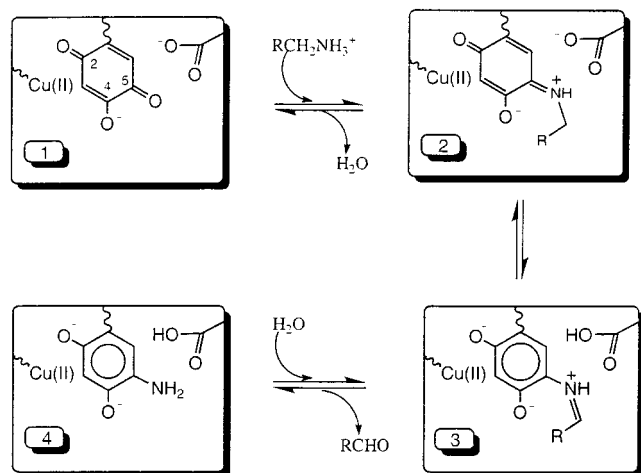


Figure 2. Experimentally suggested mechanism for the first half-reaction of copper-containing amine oxidases.

His442, His444, and His603, and to two water molecules, one equatorial and one axial in the distorted square-pyramidal geometry. The active site is deeply buried, and a significant amount of reorientation of the polypeptide is needed for the substrate to reach it. The organic cofactor TPQ and copper are in close proximity but they are not coordinated to each other with the quinone oxygen O2 (see Figure 1) lying 6 Å from the Cu atom. All three oxygen atoms of TPQ form hydrogen bonds with neighboring groups, O2 to the carboxylate side chain of Asp300, O4 to the side chain nitrogen atom of Lys296, and O5 to Tyr286 and Asn386. Asp300, Tyr286, and Asn386 residues are conserved in all the amine oxidases studied so far, whereas Lys296 is conserved in approximately half of them.²⁶ The TPQ cofactor must be highly flexible since it is required to rotate by 180° to form a Schiff base at O5 with the help of Asp300, generally believed to be an essential part of the substrate mechanism.

The most accepted mechanism for the first half-reaction of CAO^{20,27,28} is shown in Figure 2. In the first step, the substrate uses an aminotransferase mechanism to bind its nitrogen to the TPQ ring, leading to the formation of a Schiff base at the C5 position of the ring. This position is suggested on the basis of model studies with hydantoin^{29,30} and on reductive trapping experiments.^{31,32} The presence of the imine intermediate is furthermore confirmed by resonance Raman spectroscopy.¹⁴ Even more direct evidence is obtained from a crystal structure of the complex between CAO from *E. coli* and its inhibitor, 2-hydrazinopyridine, solved to 2.0 Å resolution.³³ The inhibitor does not have the C–H bond required to reach the second step, and therefore allows the isolated study of step 1. In the structure formed, the inhibitor covalently binds at the C5 position of the quinone ring of the cofactor and forms a substrate Schiff base. In the first step of the suggested mechanism, a water molecule is also formed. In the second step, a hydrogen is suggested to be abstracted from C1 of the substrate leading to a new Schiff base. Asp300 is proposed to be a likely proton abstractor in this step,^{20,25} see Figure 2, but in other suggested mechanisms Asp300 remains unprotonated after this step.³⁴ The hydrogen abstraction from C1 is indicated by kinetic isotope measurements,^{30,35} and also by recent resonance Raman spectroscopy experiments for the E406N mutant of yeast methylamine oxidase, which provide direct evidence for the accumulation of an intermediate that has all the characteristics of a product Schiff base complex.^{34,36} In the third step of the suggested mechanism, hydrolysis of the product Schiff base leads to the formation of the product aldehyde and an aminoquinol form of the cofactor.

Even though copper is not directly implied in any of the suggested steps in the first half-reaction, it is required also in this part of the reaction in all CAOs except lentil seedling amine oxidase.^{37,38} However, it should be noted that copper depletion decreases the rate of the lentil seedling amine oxidase reaction with hydrazines, which are substrate-like inhibitors.³⁸

The above detailed information about the different steps and intermediates in the catalytic cycle of CAO, combined with the known X-ray structure, provides an ideal starting point for a quantum chemical study of the mechanism. Besides giving detailed energetics for the reaction steps which can be used to test the suggested mechanism, calculations can provide additional information such as structures for short-lived intermediates and transition states. The present study is similar to previous ones, which have successfully elucidated the substrate mechanisms of ribonucleotide reductase (RNR)^{39,40} and pyruvate formate lyase (PFL).⁴¹

II. Computational Details

The calculations were performed in two steps. First, an optimization of the geometry was made using the B3LYP method⁴² with double- ζ (d95) basis sets in most cases. In the second step the B3LYP energy was evaluated for the optimized geometry using the large 6-311+G(2d,2p) basis sets, which include diffuse functions and two polarization functions on each atom. All degrees of freedom were optimized. The transition states obtained were confirmed to have only one imaginary frequency of the Hessian. Zero-point vibrational effects and thermal effects were added based on B3LYP calculations using the same basis sets as for the geometry optimization. The dielectric effects from the surrounding environment were obtained using the self-consistent isodensity polarized continuum model (SCI-PCM),⁴³ where the solute cavity is determined self-consistently. The dielectric constant was set equal to 4, which corresponds to a dielectric constant of about 3 for the protein and 80 for the water medium surrounding the protein.⁴⁴ Since models with the same charge (neutral models) were used throughout the present study, the relative dielectric effects were found to be rather small and not very sensitive to the method used or to the value chosen for the dielectric constant. The relative energies discussed below are Gibbs free energies where all the effects described above are added. Normal errors of using B3LYP and different aspects of modeling enzyme active sites are described in recent reviews.^{45,46} All calculations were performed using the GAUSSIAN-94 program.⁴⁷

To test the accuracy of the B3LYP method for the present systems, a few calculations were done at a higher level for the overall reaction energy of the reductive half-reaction. The method used for these tests was the G2MS method,⁴⁸ which is similar to the original G2MP2 method⁴⁹ except that somewhat smaller basis sets are used, the 6-31G* basis for the CCSD(T) calculations and the 6-311+G(2df,2p) basis for the MP2 calculations. B3LYP geometries as described above for the smallest possible model was used. The results are given in Table 1 and show that the reaction energy for the entire first half-reaction is 2.0 kcal/mol larger at the G2MS level than at the B3LYP level for the same model with the basis set described above, which is a quite satisfactory deviation. Zero-point, thermal, and dielectric effects are not included in this comparison.

III. Results and Discussion

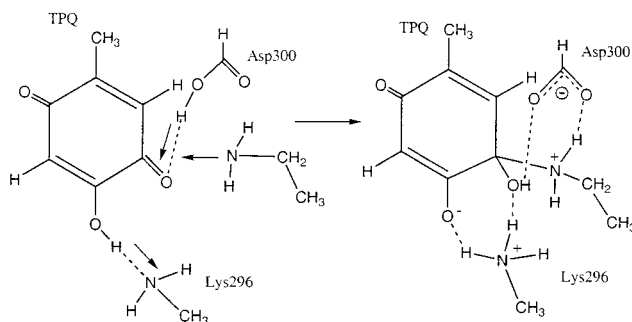
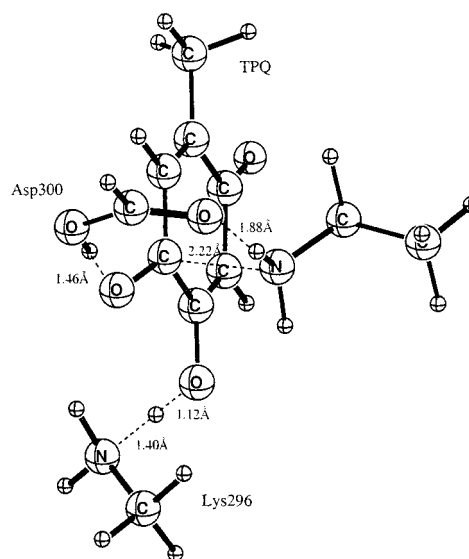
The mechanism suggested based on experiments, shown in Figure 2, was used as a starting point for the present B3LYP

TABLE 1: B3LYP and G2MS Energies (au) for the Reactants and Products of the Reductive Half-Reaction of Amine Oxidase

	E_{B3LYP}	E_{G2MS}
reactants		
TPQ (start)	-456.8091	-455.9130
methylamine	-95.8965	-95.6802
products		
TPQ (final)	-438.1894	-437.3014
formaldehyde	-114.5428	-114.3216

study of the first half-reaction (eq 1) for PSAO. The initial question to be considered here is the choice of an appropriate model for the active site including the substrate amine. It can first be concluded that since experiments suggest that the copper complex is unlikely to play a major role in this part of the reaction,³⁸ it can be left out of the model. Now what remains is to decide upon the choice of amino acid residues that need to be included in the model and the total charge state of the model. A model of Asp300 is obviously needed based on what is known experimentally. After considerable experimentation, it was decided that a model of Lys296 of PSAO is also useful for some of the steps. Since, in other CAOs, the lysine is too far away from TPQ to be likely to be active in the reactions, the role of lysine could possibly be taken either by a water or by an asparagine for these enzymes. In some steps discussed below, water and asparagine were therefore used instead of lysine to investigate the difference between these groups on the reaction. The asparagine residue has been suggested to be important for the initial positioning of the TPQ cofactor,⁵⁰ but this does not exclude also other roles for this residue. Concerning the not-so-critical charge state of the model, a neutral model was considered to be the most reasonable choice for a molecular system deeply buried in the low-dielectric of a protein. Assuming the substrate to be neutral and that Asp300 and Lys296 together carry a net neutral charge, the TPQ cofactor will then start out neutral in the first geometry optimization. It should be pointed out that this initial choice does not necessarily mean that the TPQ cofactor will always stay neutral. For some of the structures a negative TPQ cofactor was found, in line with suggestions by experiments.²⁹ For a neutral TPQ cofactor one of the three oxo groups should be protonated. By far the most stable position to protonate TPQ is at O4. The energy preference for protonating O4 compared to O2 is as large as 12 kcal/mol, and O4 therefore starts out protonated in the reaction sequence discussed below. In step 3 of this reaction mechanism, the proton is suggested to move from O4 to O2, and for this purpose three water molecules are added to the model for this step. Two of these waters are seen in the crystal structure (W_{axial} and W),⁵¹ while the third water is used to model Tyr286. In steps 2 and 5 of the suggested reaction mechanism, it was also found to be necessary to include an external water molecule in order to bridge different protonation sites. Water molecules not needed for a step were left out of the model in that step. On the basis of earlier experience, a neutral Asp300 is modeled by a formic acid, while a neutral Lys296 is modeled by a methylamine. The neutral substrate is modeled by an ethylamine.

a. Step 1: Substrate Attack at the C5 Site of TPQ. As a starting point for the geometry optimization for the first step of the amine oxidation in PSAO all the different species involved, Lys296, Asp300, TPQ, and the substrate, were chosen neutral. The optimization of the reactant did not change the charge states of any of the amino acids involved, nor of TPQ or the substrate. The best present suggestion for the first step is shown in Figure 3. This step can be described as a simultaneous protonation of O5 of TPQ by the neutral aspartate, and an attack of the amine

**Figure 3.** Suggested first step of the amine oxidation in PSAO.**Figure 4.** Optimized transition state for step 1.

of the substrate on C5. A concerted attack on C5 and O5 is necessary for a low barrier. This step has large similarities to one of the steps suggested for the RNR substrate reaction sequence, where a ketogroup is attacked by a cysteine and a carboxylate³⁹ and is probably a quite general mechanism for these types of reactions. Besides the attack on C5 a proton also moves from O4 to Lys296, so that at the end of this step both Lys296 and Asp300 are charged and the TPQ cofactor is negative. The step illustrated in Figure 3 is found to have only a small barrier of 2.6 kcal/mol and to be perfectly thermoneutral. The transition state obtained is shown in Figure 4. The calculated entropy effect is +4.0 kcal/mol (included in the values), favoring the reactants and indicating a more tightly bound product than reactant. On the other hand, the dielectric effect (also included in the values) favors the products by 4.0 kcal/mol, and is due to the formation of the charged residues indicated in the figure.

b. Step 2: Formation of the Substrate Schiff Base. The suggested second step of the reaction mechanism is divided into two parts, shown in Figure 5 and Figure 6, and describes the formation of the substrate Schiff base observed experimentally in a crystal structure of the *E. coli* enzyme with the 2-hydrazinopyridine inhibitor.³³ It has also been observed by resonance Raman,¹⁴ in model studies,^{29,30} and by reductive trapping experiments.^{31,32} The formation of this base is suggested to involve a proton transfer from the amino group over a solvent water molecule to the C5 hydroxyl group, where a water molecule is released. In the first part of this reaction step the substrate amino group is deprotonated and Asp300 is protonated in a proton-transfer chain reaction. This part has a barrier of 15.1 kcal/mol, which includes zero-point vibrational (plus thermal enthalpy) effects of +3.3 kcal/mol and dielectric effects

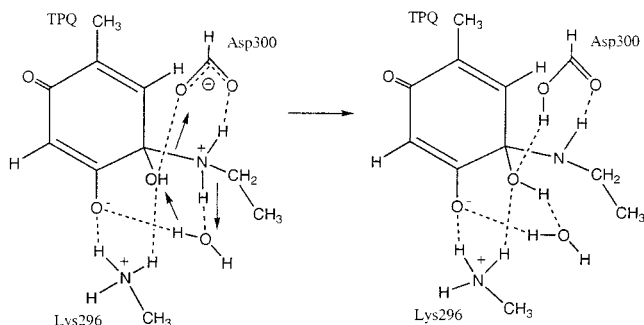


Figure 5. Suggested first part of the second step of the amine oxidation in PSAO.

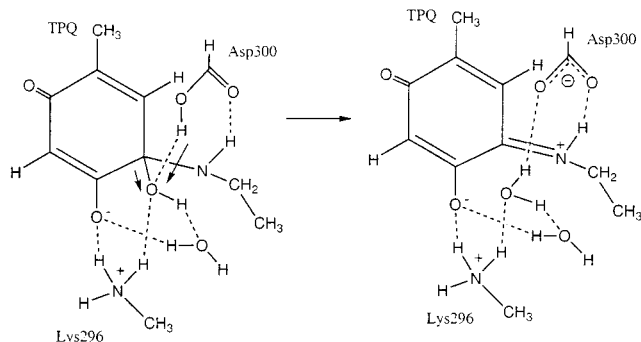


Figure 6. Suggested second part of the second step of the amine oxidation in PSAO.

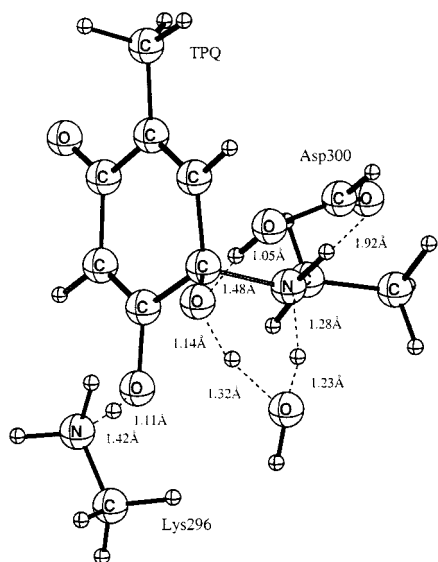


Figure 7. Optimized transition state for the first part of step 2.

of -2.3 kcal/mol, and it is uphill by 5.5 kcal/mol. The transition state obtained is shown in Figure 7. In this transition state structure it may appear as if a proton was also moving between Lys296 and O4 in this step, but this is not the case. The proton position is essentially the same from reactant to product. After this step the main reaction coordinate is the C–O bond between the C5 carbon and the water molecule being formed. Simultaneously Asp300 is deprotonated again. The resulting transition state is shown in Figure 8. The computed barrier for this part is 8.1 kcal/mol, which includes zero-point vibrational (plus thermal enthalpy) effects of $+0.5$ kcal/mol and dielectric effects of -0.1 kcal/mol. Going from reactants to products in step 2 is exothermic by 2.5 kcal/mol, where zero-point vibrational (plus thermal enthalpy) effects contribute -0.2 kcal/mol and dielectric effects -1.1 kcal/mol. The calculated entropy effect is -3.5

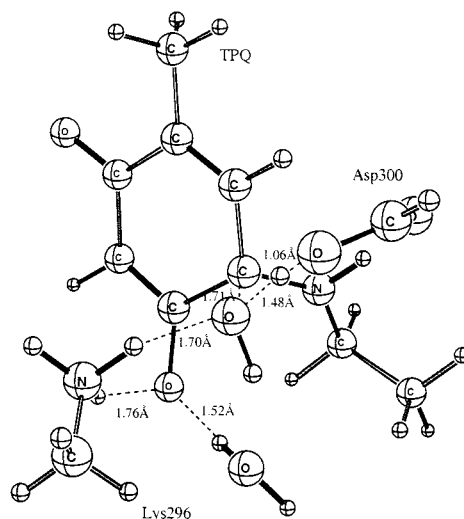


Figure 8. Optimized transition state for the second part of step 2.

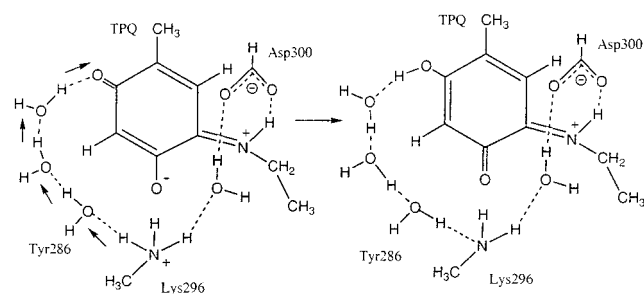


Figure 9. Suggested first part of the third step of the amine oxidation in PSAO.

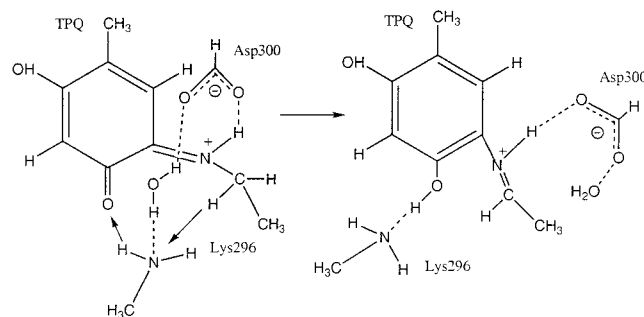


Figure 10. Suggested second part of the third step of the amine oxidation in PSAO.

kcal/mol (included in the values) favoring the product, and is due to the release of the water molecule. The fact that the second step is calculated to be exothermic agrees with the inhibitor crystal structure of the enzyme which shows that the doubly bonded substrate Schiff base is more stable than the singly bonded reactant of this step.

c. Step 3: Formation of the Product Schiff Base. The suggested step 3 is also divided into two parts, which are shown in Figure 9 and Figure 10. This is a key step of the entire mechanism in which the C–H bond of the substrate is broken. A second Schiff base is formed in this step which can be identified with the product Schiff base recently observed by resonance Raman spectroscopy of a mutant of yeast methylamine oxidase.^{34,36} To accomplish the difficult task of breaking the C–H bond, full use has to be made of resonance effects in the TPQ ring. This requires that O2 of TPQ becomes protonated before the C–H activation, and a suggestion for how this is done in PSAO is shown as the first part of the third step in

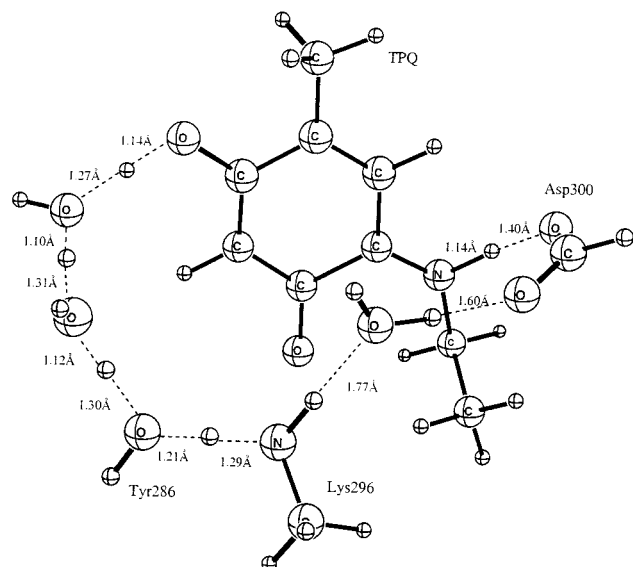


Figure 11. Optimized transition state for the first part of the third step of the amine oxidation in PSAO.

Figure 9. A proton is initially available at Lys296, but a rather long-range proton transfer is needed for it to reach O₂. It turns out that the enzyme is perfectly set up for this transfer, with a hydrogen-bonded chain composed of Tyr286 and the two water molecules observed in high-resolution structures of amine oxidases.^{51,52} It is interesting to note that the enzyme is likely to make use of this hydrogen-bonded chain also in the oxidative half-reaction where hydrogen peroxide is formed from an oxygen molecule. The optimized transition state for the proton transfer to O₂ is shown in Figure 11. This part of the third step is endothermic by 8.1 kcal/mol, where entropy effects contribute -0.6 kcal/mol and dielectric effects -1.6 kcal/mol. The barrier for the proton to reach O₂ is 10.1 kcal/mol, where zero-point vibrational (plus thermal enthalpy) effects lower the barrier significantly by 5.4 kcal/mol. Entropy and dielectric effects on the barrier are $+0.7$ kcal/mol and -1.1 kcal/mol, respectively. With the proton present at O₂, the enzyme is well prepared to perform the C–H bond breaking. This is done in the second half of the third step and is driven by a strong exothermicity of 28.5 kcal/mol, which mainly comes from the aromaticity of the TPQ ring obtained in this step. It is interesting to note that textbook values for the energy gain by aromaticity is 36 kcal/mol,⁵³ based on the hydrogenation energy of benzene, which is rather close to the exothermicity in this step. However, if the ring is replaced by hydrogen atoms bound to C4 and C5, thereby destroying the gain obtained by the aromaticity, the exothermicity decreases by only 19 kcal/mol. The entropy effects increase the exothermicity by 1.9 kcal/mol, and the dielectric effects give an increase by 2.3 kcal/mol. It is clearly highly significant that the enzyme places almost all of the available reaction exothermicity from the reductive half-reaction in this single critical step where the C–H bond is broken, since this is a way to bring down the barrier and increase the rate. The possibility to use the aromaticity as a driving force in the rate-determining step is obviously the reason the enzyme has a quinone as a cofactor. The situation described here is quite similar to manganese catalase, which was recently studied by similar methods,⁵⁴ where almost all of the available exothermicity was found to be placed in the single rate-limiting step where the O–O bond is broken, and is probably common for enzyme-catalyzed reactions in general. The transition state for this step is shown in Figure 12. In the present mechanism Asp300 remains unprotonated in this step in agreement with

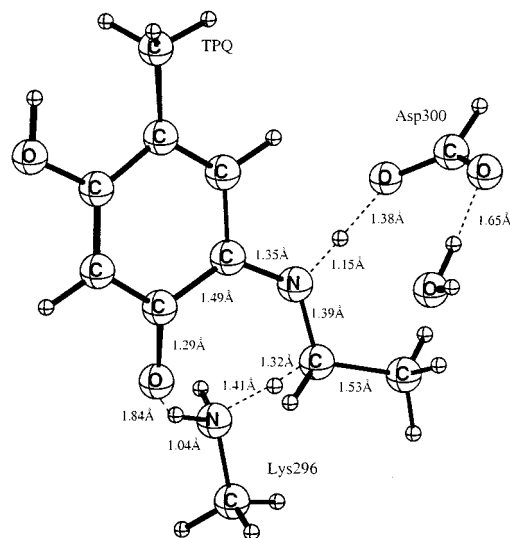


Figure 12. Optimized transition state for the second part of the third step of the amine oxidation in PSAO.

some experimental suggestions³⁴ (see Introduction), but does form a very strong hydrogen bond with a distance of only 1.38 Å. The water molecule produced in step 2, is hydrogen bonded to the second oxygen of the Asp300 carboxylate, and swings around in this process, and is then prepared for the next step placed close to the substrate C1 carbon. This happens automatically in the geometry optimization. The barrier for this step is 8.4 kcal/mol, which includes zero-point vibrational (plus thermal enthalpy) effects of 3.7 kcal/mol, entropy effects of -0.1 kcal/mol, and dielectric effects of $+2.3$ kcal/mol. The origin of the large dielectric effect is a large change of dipole moment from 3.3 D for the reactant to 7.1 D for the transition state structure. Since the third step follows a step which is endothermic by 8.1 kcal/mol (see above), the barrier to break the C–H bond becomes 16.5 kcal/mol. This barrier makes it the rate-limiting step of the presently suggested mechanism for the reductive half-reaction, which agrees well with rapid scanning kinetic data.⁵⁵ The calculated kinetic isotope effect is 3.9 (by substituting hydrogen by deuterium on the CH₂ group of the substrate), which is significant but still lower than the experimental isotope effect of 8.5. This type of underestimation is common and could at least partly be due to tunneling effects⁵⁶ not included in the present estimate. As a final comment on this step, it can be noted that lysine is assigned an important role as proton donor in the first half of this step and as a proton-transfer agent in the second part. Since lysine is not as close to the active site in other CAOs its roles might be taken by other residues for those enzymes. It is difficult to predict where the proton needed at O₂ comes from in the other CAOs. A proton source other than the lysine appears likely since it is 7.5 Å away from O₄ in *H. polymorpha*.¹⁶ As a proton transfer agent in the second part its role definitely has to be taken over by some other molecule. Replacing lysine with water increases the barrier for the second part by as much as 7.3 kcal/mol, but using both water and asparagine, leads to a barrier which is only 1.5 kcal/mol higher than the one with lysine. To the accuracy of the present methods these barriers are therefore essentially the same.

d. Step 4: Substrate C–OH Bond Formation. In the suggested fourth step, the water molecule formed in step 2 attacks the C1 carbon of the substrate, see Figure 13. After step 2, the water molecule is bound to one of the oxygens of the Asp300 carboxylate, but in the course of step 3, the Asp300 has swung around 180° (see above) and thereby positioned the water in the region of the C1 of the substrate. Since Lys296

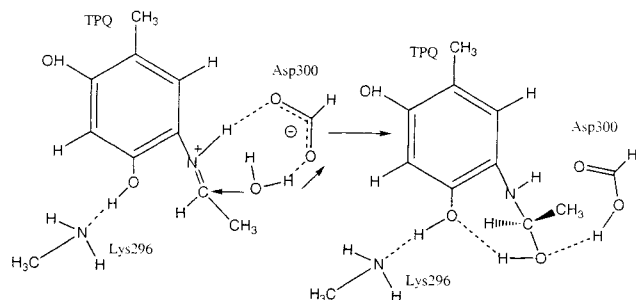


Figure 13. Suggested fourth step of the amine oxidation in PSAO.

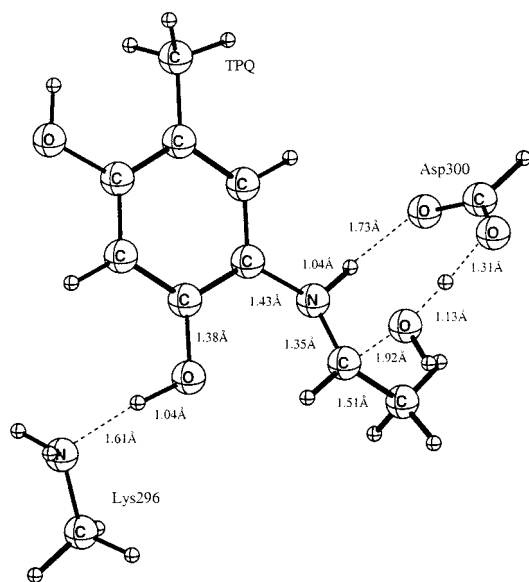


Figure 14. Optimized transition state for step 4.

has become hydrogen bonded to the O4 hydroxyl group, which is reasonably far away from the substrate, it is not active in this step. The transition state for formation of the substrate C–O bond is shown in Figure 14. The calculated barrier is 11.8 kcal/mol, to which entropy effects contribute by +2.3 kcal/mol. The reason for this is that there is a relatively free water molecule before the reaction with a large entropy. Dielectric effects are small, raising the barrier by 0.6 kcal/mol. Asp300 plays a crucial role in the C–O bond formation as proton abstractor from the water molecule. In fact, this is the most important function of this aspartate so far in the present mechanism for the reductive half-reaction. This result agrees well with mutation experiments on yeast methylamine oxidase,^{34,36} which show that if Asp319 (which corresponds to Asp300 in PSAO) is replaced by an asparagine, the reductive half-reaction will halt after the formation of the product Schiff base (the third step, see above). The C–O formation step is endothermic by 3.1 kcal/mol, where again entropy contributes significantly by +2.7 kcal/mol for the same reason as for the barrier. For the reaction energy, solvent effects are more important than for the barrier, increasing the endothermicity by 2.3 kcal/mol. The reason is a change of dipole moment from 11.5 to 6.5 D for the products.

e. Step 5: Transfer of Proton from Asp300 to Substrate Nitrogen. In the suggested fifth step, a proton should be moved from the carboxylate of Asp300 to the substrate nitrogen. This might appear as a rather simple step. All that is required is that the Asp300 swings around 180°, as it did during the third step, and delivers the proton to the substrate nitrogen. However, the barrier for rotating Asp300 is prohibitively high. The reason is that the hydrogen bond to the substrate hydroxyl group is very

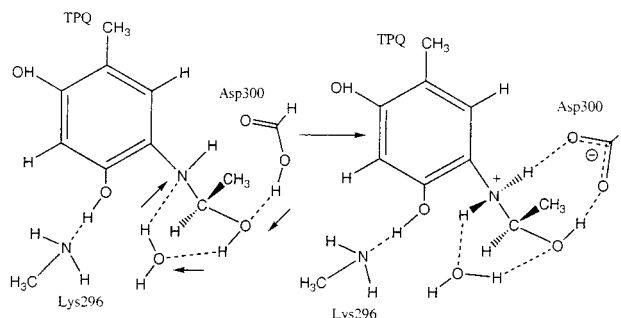


Figure 15. Suggested fifth step of the amine oxidation in PSAO.

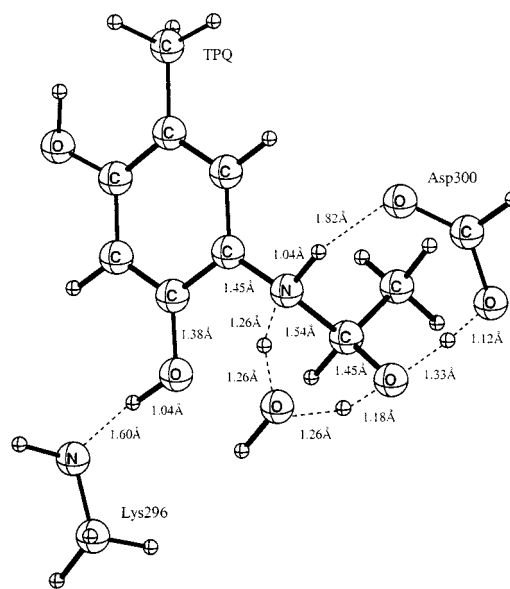


Figure 16. Optimized transition state for step 5.

strong with a short O–H distance of only 1.45 Å. A large number of attempts were required before the suggestion depicted in Figure 15 was found. In this mechanism, which requires an added water molecule, a proton is transferred from the aspartic acid over the water molecule to the nitrogen, rather than by a direct rotation of Asp300. The optimized transition state is shown in Figure 16. As seen in this figure, the proton transfer is a strongly concerted process with several O–H and N–H distances in the range 1.1–1.3 Å. The computed barrier height is 10.6 kcal/mol, where zero-point vibrational (plus thermal enthalpy) effects have lowered the barrier significantly by 4.1 kcal/mol. Entropy and solvation effects on the barrier are small. The fifth reaction step is weakly exothermic by 0.5 kcal/mol. A final model calculation was done for step 5 in which lysine replaces the water molecule in transferring the proton. This turned out to be less favorable and led to an increase of the barrier for this step by 4 kcal/mol.

f. Step 6: Formation of Product Aldehyde. The only step remaining in the first half-reaction is the sixth one which should release the product aldehyde. The suggested mechanism is shown in Figure 17. The water molecule which was added in step 5 is no longer needed and is therefore removed from the model. To break the C–N bond of the substrate to release the aldehyde, a proton transfer to Asp300 is needed. This is another important function of Asp300 in the reductive half-reaction. As discussed above, Asp300 is also crucial in steps 4 and 5 as proton abstractor and donor. No transition state for product release was found in step 6, but the reaction is only uphill by 5.9 kcal/mol. The reason the transition state optimization failed even though explicit Hessians were calculated, is due to a very

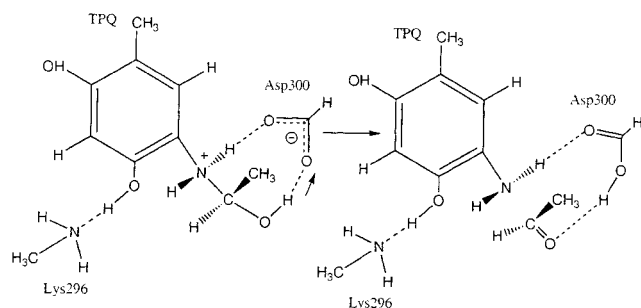


Figure 17. Suggested sixth step of the amine oxidation in PSAO.

small barrier for the backward reaction which led the geometry optimization either to the reactant or to the product. However, a small barrier for this step should have almost no chemical consequences. Rather surprisingly, the calculated entropy effect on the endothermicity is only 0.3 kcal/mol. One reason for this is that there is a very strong hydrogen bond between the product aldehyde released and Asp300 (1.59 Å). It is clear that as this hydrogen bond is replaced by hydrogen bonds to other residues, the aspartate will be deprotonated. In this process, the aldehyde would become much more free and a gain of entropy would result that together with the deprotonation of Asp300 should eventually make this step exothermic. This part of the final step of the reductive half-reaction was not modeled here since it would require a substantially larger model than the one presently used. As the C–N bond of the substrate is broken, the cofactor is left in its aminoquinol form. It will return to its original TPQ form only after the oxidative half-reaction.

IV. Conclusions

The reductive half-reaction of PSAO has been studied by similar computational methods and models as have been used previously for the substrate reactions of other enzymes such as

RNR and PFL. As usual, the present investigation was strongly guided by experimental structural and spectroscopic information, which is summarized in the mechanism shown in Figure 2. The energy diagrams for the presently suggested PSAO mechanism can be divided into six steps, as shown in Figures 18 and 19. Two of these steps are further subdivided into two steps each. Energy diagrams were constructed by imposing that the reactant of each step has the same energy as the product of the previous step. There is one exception to this rule and this is for step 5. In this case the product of step 5 is placed at a calculated energy of 0.4 kcal/mol below the reactant of step 4. The reason for this is that in step 5 there is an addition of an extra water molecule, while in the fourth and sixth step the same size of models were used. The reactant of the sixth step was found to be 0.4 kcal/mol lower than the reactant of the fourth step using the same model. By placing the product of step 5 below the reactant of step 4 a minor discrepancy to experiment was avoided, since it is known that the reactant of step 6 should be lower than the reactant of step 4. The calculated energies are given in Table 2.

The first step in the presently suggested scheme is the thermoneutral addition of the amine substrate to the C5 carbon of TPQ, which occurs simultaneously as O5 becomes protonated by Asp300. There is a small barrier of 2.6 kcal/mol for this step. In the second step, the O5 hydroxyl group of TPQ, formed in step 1, becomes protonated to form a water molecule. In the first part of this step there is a proton transfer from the substrate, over an external water and the O5 hydroxyl group to Asp300. This part is endothermic by 5.5 kcal/mol and goes over a barrier of 15.1 kcal/mol. The product of the second part of this step is the substrate Schiff base observed experimentally in a crystal structure with an inhibitor³³ and by resonance Raman spectroscopy.¹⁴ The second part goes over a barrier of 8.1 kcal/mol and is exothermic by 8.0 kcal/mol. Overall, this makes the second step slightly exothermic by 2.5 kcal/mol, which is in agreement

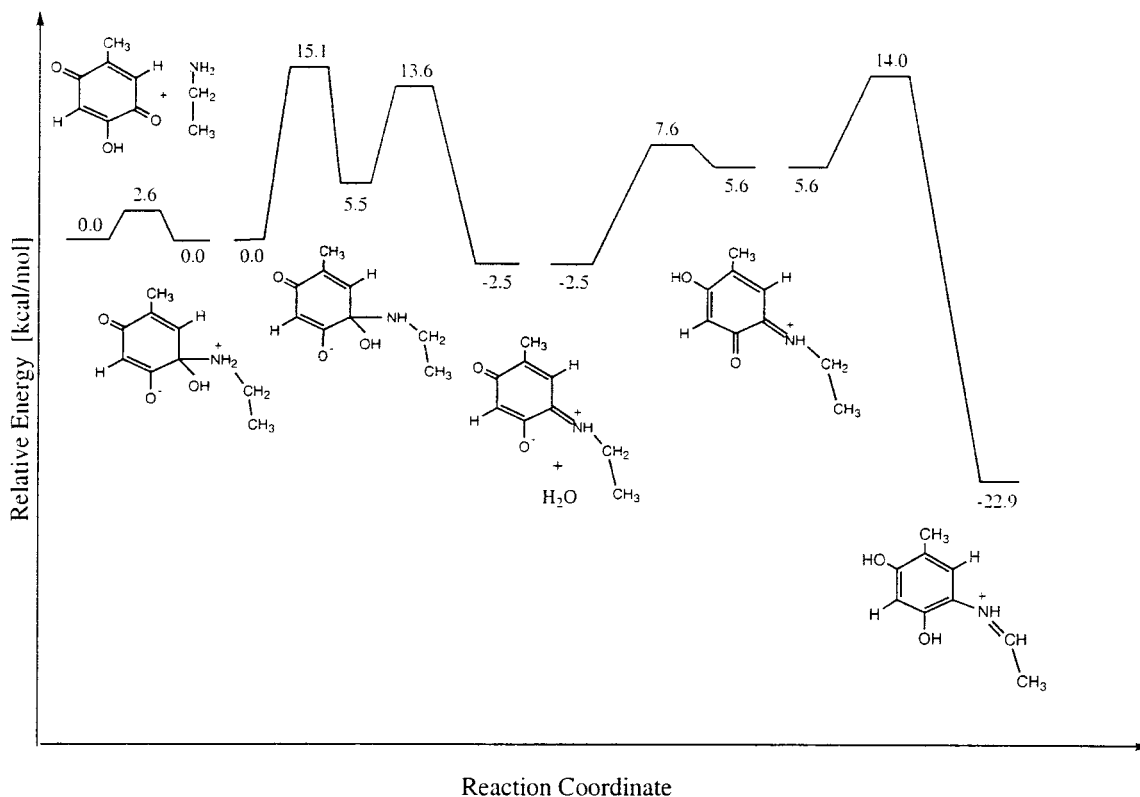


Figure 18. Energy diagram for the first three steps of the reductive half reaction of PSAO.

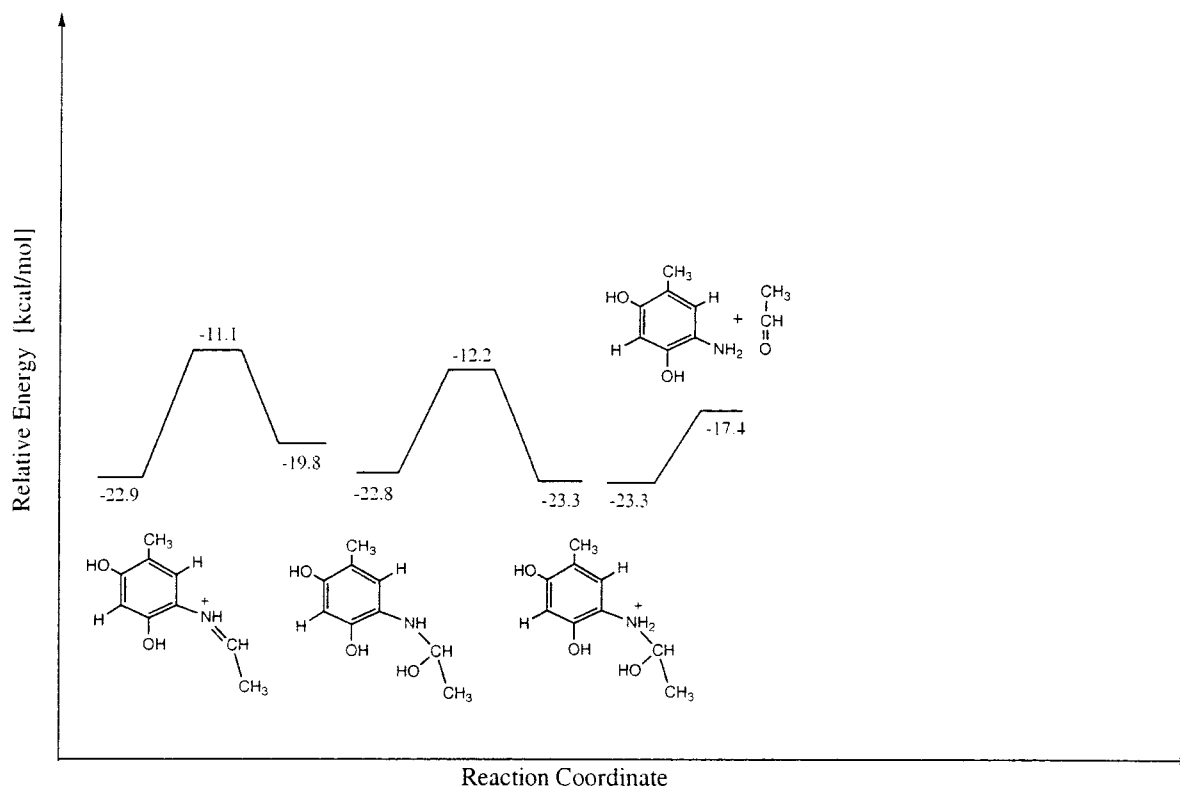


Figure 19. Energy diagram for the last three steps of the reductive half reaction of PSAO.

TABLE 2: Energies (au) for the Optimized Structures of the Different Steps

	$E_{\text{big basis}}$	E_{DZ}	$E_{\Delta H}^a$	E_{solv}^b	$E_{T\Delta S}$
Step-1					
R	-917.1428	-916.7261	0.3359	-916.7397	0.0788
TS	-917.1405	-916.7266	0.3351	-916.7407	0.0756
P	-917.1411	-916.7402	0.3376	-916.7602	0.0725
Step-2a					
R	-993.6127	-993.1834	0.3639	-993.2031	0.0752
TS	-993.5857	-993.1499	0.3587	-993.1660	0.0764
P	-993.5994	-993.1557	0.3655	-993.1754	0.0781
Step-2b					
R	-993.5994	-993.1557	0.3655	-993.1754	0.0781
TS	-993.5882	-993.1522	0.3647	-993.1717	0.0757
P	-993.6132	-993.1826	0.3637	-993.2005	0.0808
Step-3a					
R	-1146.5769	-1146.0819	0.4194	-1146.0985	0.0914
TS	-1146.5551	-1146.0699	0.4109	-1146.0847	0.0903
P	-1146.5578	-1146.0984	0.4167	-1146.1010	0.0924
Step-3b					
R	-917.1242	-916.7078	0.3355	-916.7229	0.0772
TS	-917.1012	-916.6856	0.3296	-916.7043	0.0773
P	-917.1633	-916.7496	0.3357	-916.7684	0.0802
Step-4					
R	-917.1633	-916.7496	0.3357	-916.7684	0.0802
TS	-917.1482	-916.7395	0.3347	-916.7574	0.0765
P	-917.1691	-916.7589	0.3383	-916.7740	0.0759
Step-5					
R	-993.6403	-993.1896	0.3657	-993.2062	0.0788
TS	-993.6164	-993.1801	0.3591	-993.1974	0.0785
P	-993.6424	-993.1971	0.3646	-993.2151	0.0749
Step-6					
R	-917.1698	-916.7568	0.3378	-916.7759	0.0761
P	-917.1610	-916.7406	0.3353	-916.7561	0.0766

^a The sum of zero-point and thermal enthalpy effects. ^b Calculated with DZ basis set.

with the fact that the substrate Schiff base is the one observed experimentally and not the singly bonded reactant of this step.

The third step of the reductive half-reaction is the most critical one and is rate-limiting in the present model in agreement with experiments.⁵⁵ This step is also subdivided into two parts. In the first part a proton is transferred from Lys296 hydrogen bonded to O4 over to O2 using a hydrogen-bonded chain of two waters and one tyrosine, all of them observed at proper positions in the X-ray structures. This part is endothermic by 8.1 kcal/mol and goes over a barrier of 10.1 kcal/mol. In the second part of this step a C–H bond of the substrate is broken and the O4 of TPQ becomes protonated. The proton is suggested to be transferred over Lys296 in PSAO while in other CAOs the role of lysine could be taken by a water molecule assisted by an asparagine. Asp300 is only a spectator in the present mechanism and remains unprotonated in agreement with some previous suggestions.³⁴ The second part of this step is strongly exothermic by 28.5 kcal/mol which helps in overcoming the C–H bond cleavage barrier. A large part, 19 kcal/mol, of this exothermicity comes from the aromaticity introduced into the quinone ring. The overall barrier for step 3 is calculated to be 16.5 kcal/mol. The product is a second Schiff base, which has also been observed experimentally by resonance Raman spectroscopy for an E406N mutant of yeast methylamine oxidase.^{34,36} The reason this product Schiff base can be observed is that Asp319 (corresponding to Asp300 in PSAO) plays a key role in the next step, where the substrate is hydroxylated, and its removal therefore prevents this step. In step 5 the substrate is protonated by Asp300 in step 5. Since Asp300 is locked in its position from step 4, an external solvent water molecule is needed to assist in the proton transfer. The barriers for step 4 of 11.8 kcal/mol and for step 5 of 10.6 kcal/mol are substantially lower than for the rate-limiting step 3. Finally, in step 6 the aldehyde is released. The present mechanism, as described in Figure 18 and Figure 19, agrees very well with most of the available experimental information. In addition the calculations supply information about the energetics of the different reaction

steps as well as detailed transition state structures and should be useful for further analysis of this interesting enzyme reaction.

References and Notes

- McIntire, W. S.; Hartmann, C. Copper containing amine oxidases. In *Principles and application of quinoproteins*; Davidson, V. L., Ed; Marcel Dekker: New York, 1993; pp 97–171.
- Klinman, J. P.; Mu, D. *Annu. Rev. Biochem.* **1994**, *63*, 299–344.
- McIntire, W. S. *Annu. Rev. Nutr.* **1998**, *18*, 145–177.
- Möller, S. G.; McPherson, M. J. *Plant J.* **1998**, *13*, 781–791.
- Knowles, P. F.; Dooley, D. M. In *Metal ions in biological systems*; Sigel, H., Sigel, A., Eds.; Marcel Dekker: New York, 1994; *30*, p 361.
- Bono, P.; Salmi, M.; Smith, D. J.; Jalkanen, S. *J. Immunol.* **1998**, *160*, 5563–5571.
- Boomsma, F.; vanVeldhuisen, D. J.; deKam, P. J.; ManintVeld, A. J.; Mosterd, A.; Lie, K. I.; Schalekamp, M. *Cardiovasc. Res.* **1997**, *33*, 387–391.
- Murray, J. M.; Saysell, C. G.; Wilmot, C. M.; Tambyrajah, W. S.; Jaeger, J.; Knowles, P. F.; Phillips, S. E. V.; and McPherson, M. J. *Biochemistry* **1999**, *38*, 8217–8227.
- McIntire, W. S. *FASEB J.* **1994**, *8*, 513.
- Tanizawa, K. *J. Biochem.* **1995**, *118*, 671–678.
- Janes, S. M.; Klinman, J. P. *Biochemistry* **1991**, *30*, 4599–4605.
- Janes, S. M.; Palcic, M. M.; Scaman, C. H.; Smith, A. J.; Brown, D. E.; Dooley, D. M.; Mure, M.; Klinman, J. P. *Biochemistry* **1992**, *31*, 12147–12154.
- Cooper, R. A.; Knowles, P. F.; Brown, D. E.; McGuirl, M. A.; Dooley, D. M. *Biochem. J.* **1991**, *288*, 337–340.
- Brown, D. E.; McGuirl, M. A.; Dooley, D. M.; Janes, S. M.; Mu, D.; Klinman, J. P. *J. Biol. Chem.* **1991**, *266*, 4049–4051.
- Janes, S. M.; Mu, D.; Smith, A. J.; Kaur, S.; Maltby, D.; Burlingame, A. L.; Klinman, J. P. *Science* **1990**, *248*, 981–987.
- Mu, D.; Janes, S. M.; Smith, A. J.; Brown, D. E.; Dooley, D. M.; Klinman, J. P. *J. Biol. Chem.* **1992**, *267*, 7979–7982.
- Cai, D.; Klinman, J. P. *J. Biol. Chem.* **1994**, *269*, 32039–32042.
- Matsuzaki, R.; Fukui, T.; Sato, H.; Ozaki, Y.; Tanizawa, K. *FEBS Lett.* **1994**, *351*, 360–364.
- Klinman, J. P. *Chem. Rev.* **1996**, *96*, 2541–2561.
- Stubbe, J.; Van der donk, W. A. *Chem. Rev.* **1998**, *98*, 705–762.
- Knowles, P. F.; Yadav, D. S. *Copper Proteins and Copper Enzymes*; Lontie, R., Ed.; CRC Press: Boca Raton, 1984; p 103.
- Palcic, M. M.; Klinman, J. P. *Biochemistry* **1983**, *22*, 5957.
- Lindström, A.; Petterson, G. *Eur. J. Biochem.* **1978**, *84*, 479–485.
- Rius, F. X.; Knowles, P. F.; Petterson, G. *Biochem. J.* **1984**, *220*, 767–772.
- Kumar, V.; Dooley, D. M.; Freeman, C. H.; Guss, J. M.; Harvy, I.; McGuirl, M. A.; Wilce, M. C. J.; Zubak, V. M. *Structure* **1996**, *4*, 943–955.
- Tipping, A. J.; McPherson, M. J. *J. Biol. Chem.* **1995**, *270*, 16939–16946.
- Hartmann, C.; Klinman, J. P. *Biochemistry* **1991**, *30*, 4605–4611.
- Bellelli, A.; Finnazi-Agró, A.; Floris, G.; Brunori, M. *J. Biol. Chem.* **1991**, *266*, 20654–20657.
- Mure, M.; Klinman, J. P. *J. Am. Chem. Soc.* **1993**, *115*, 7117–7127.
- Mure, M.; Klinman, J. P. *J. Am. Chem. Soc.* **1995**, *117*, 8707–8718.
- Hartmann, C.; Klinman, J. P. *J. Biol. Chem.* **1987**, *262*, 962–965.
- Hartmann, C.; Klinman, J. P. *FEBS Lett.* **1990**, *261*, 441–444.
- Wilmot, C. M.; Murray, J. M.; Gordon, A.; Parsons, M. R.; Convery, M. A.; Blakeley, V.; Corner, A. S.; Palcic, M. M.; Knowles, P. F.; McPherson, M. J.; Phillips, S. E. V. *Biochemistry* **1997**, *36*, 1608–1620.
- Cai, D.; Dove, J.; Nakamura, N.; Sanders-Loehr, J.; Klinman, J. P. *Biochemistry* **1997**, *36*, 11472–11478.
- Mure, M.; Klinman, J. P. *J. Am. Chem. Soc.* **1995**, *117*, 8698–8706.
- Klinman, J. P. *J. Biol. Chem.* **1996**, *271*, 27189–27192.
- Rinaldi, A.; Giartosio, A.; Floris, G.; Medda, R.; Finnazi-Agró, A. *Biochem. Biophys. Res. Commun.* **1984**, *120*, 242–249.
- Medda, R.; Padiglia, A.; Pedersen, J. Z.; Rotilio, G.; Agró, A. F.; Floris, G. *Biochemistry* **1995**, *34*, 16375–16381.
- Siegbahn, P. E. M. *J. Am. Chem. Soc.* **1998**, *120*, 8417–8429.
- Himo, F.; Siegbahn, P. E. M. *J. Phys. Chem. B* **2000**, *104*, 7502–7509.
- Himo, F.; Eriksson, L. A. *J. Am. Chem. Soc.* **1998**, *120*, 11449–11455.
- Becke, A. D. *Phys. Rev.* **1988**, *A38*, 3098; Becke, A. D. *J. Chem. Phys.* **1993**, *98*, 1372; Becke, A. D. *J. Chem. Phys.* **1993**, *98*, 5648.
- Wiberg, K. A.; Keith, T. A.; Frisch, M. J.; Murcko, M. *J. Phys. Chem.* **1995**, *99*, 9072.
- Blomberg, M. R. A.; Siegbahn, P. E. M.; Babcock, G. T. *J. Am. Chem. Soc.* **1998**, *120*, 8812–8824.
- Siegbahn, P. E. M.; Blomberg, M. R. A. *Annu. Rev. Phys. Chem.* **1999**, *50*, 221–249.
- Siegbahn, P. E. M.; Blomberg, M. R. A. *Chem. Rev.* **2000**, *100*, 421–437.
- Frisch, M. J.; Trucks, G. W.; Schlegel, H. B.; Gill, P. M. W.; Johnson, B. G.; Robb, M. A.; Cheeseman, J. R.; Keith, T.; Petersson, G. A.; Montgomery, J. A.; Raghavachari, K.; Al-Laham, M. A.; Zakrzewski, V. G.; Ortiz, J. V.; Foresman, J. B.; Cioslowski, J.; Stefanov, B. B.; Nanayakkara, A.; Challacombe, M.; Peng, C. Y.; Ayala, P. Y.; Chen, W.; Wong, M. W.; Andres, J. L.; Replogle, E. S.; Gomperts, R.; Martin, R. L.; Fox, D. J.; Binkley, J. S.; Defrees, D. J.; Baker, J.; Stewart, J. P.; Head-Gordon, M.; Gonzalez, C.; Pople, J. A.; *Gaussian 94*, Revision B.2; Gaussian Inc.: Pittsburgh, PA, 1995.
- Froese, D. J.; Humbel, S.; Svensson, M.; Morokuma, K. *J. Phys. Chem.* **1997**, *101*, 227.
- Curtiss, L. A.; Raghavachari, K.; Pople, J. A. *J. Chem. Phys.* **1993**, *98*, 1293.
- Schwartz, B.; Edward, L. G.; Sanders-Loehr, J.; Klinman, J. P. *Biochemistry* **1993**, *32*, 2234–2241.
- Qiaojuan, S.; Klinman, J. P. *Biochemistry* **1998**, *37*, 12513–12535.
- Wilmot, C. M.; Hajdu, J.; McPherson, M. J.; Knowles, P. F.; Phillips, S. E. V. *Science* **1999**, *286*, 1724–1728.
- Solomons, T. W. G. *Organic Chemistry*, 4th ed.; John Wiley: New York, 1988.
- Siegbahn, P. E. M. *Theor. Chem. Acc.* **2001**, *105*, 197–206.
- Hartmann, C.; Brzovic, P.; Klinman, J. P. *Biochemistry* **1993**, *32*, 2234–2241.
- Grant, K. L.; Klinman, J. P. *Biochemistry* **1989**, *28*, 6597–6605.